Viser Technology Pte. Ltd.
Research and Application of Materials Science
DOI: 10.33142/rams.v7i1.18640

Research Article Open Access

Many-body Interaction Properties and Zero-point Vibration Pressure of Solid Argon Based on Atomic Crystal Configurations

Xingrong ZHENG*, Fengfeng YANG, Haijun CHEN

College of New energy, Longdong University, Qingyang, Gansu, 745000, China

*Corresponding Author: Xingrong ZHENG, E-mail: zhengxingrong2006@163.com

Abstract

Based on atomic crystal configurations, we studied many-body interaction properties of face-centered cubic (fcc) solid argon (Ar) within the atomic distance range of 2.0Å to 3.6Å at T=300 K. The resulting EOS can accurately describe the compression behavior of solid Ar under the experimentally investigated pressure range (0～114GPa). Statistically, 903 $(Ar)_2$ clusters were identified, corresponding to 12 distinct geometric configurations, 861(Ar)3 clusters correspond to 25 distinct geometric configurations, 816 (Ar)4 clusters correspond to 27 distinct geometric configurations, and the calculation results exhibited good convergence. For comparative purposes, the EOS of fcc solid Ar was also calculated using a two-body potential-only approach, which showed excellent agreement with experimental data under relevant pressures. Incorporating three-body terms extended the EOS accuracy to 80 GPa, while the inclusion of four-body terms further improved the precision up to 114 GPa. Higher-order many-body terms are expected to enable accurate interpretation of experimental phenomena in solid Ar above 114 GPa. In addition, when the molar volume is reduced to a fixed value, the zero-point vibration pressure has already reached a certain proportion, then it must be considered and cannot be ignored. This study provides a reliable theoretical model for the study of high-pressure properties and zero-point energy of rare gas solids.

Keywords: *Solid argon; Atomic configuration; Many-body interaction properties*

1 Introduction

Solid argon (*Ar*), as a typical rare gas solid, has attracted extensive theoretical research interest due to its unique electronic and optical properties[1-7]. It also has important application prospects in fields such as cryogenic phonon detectors[5] and dark matter detection, while zero-point vibration energy[6] and other related properties have become key research focuses. Previous studies have explored the EOS of solid *Ar* under different temperature and pressure conditions[2,7], and first-principles calculations have been widely used to analyze its electronic structure and elastic modulus [3,4]. However, the influence of multi-body interactions (especially high-order terms) on the EOS of solid *Ar* under high pressure (exceeding 80 GPa) still needs further refinement[8-15]. Recent scientific research on solid *Ar* has yielded significant advances across extreme condition chemistry, thermophysical property characterization, and applied material sciences[16-22]. A groundbreaking 2025 study by Lawrence Livermore National Laboratory and collaborators revealed that solid argon loses its chemical inertness under conditions mimicking Earth's core-pressures exceeding 1.5 million atmospheres and temperatures above 2,000 Kelvin-reacting with nickel to form a stable ArNi intermetallic compound, which may resolve longstanding geological questions about argon's fate in planetary interiors[21]. In the realm of thermophysical research, a recent study published in the Journal of Molecular Modeling has significantly refined the computational framework for predicting the transport properties of solid Ar (e.g., diffusion coefficient and viscosity). By integrating nuclear spin effects and symmetry constraints into the theoretical model, and leveraging ab initio-derived potential energy curves coupled with the Chapman-Enskog kinetic theory, this work has substantially enhanced the predictive accuracy of transport properties across a broad temperature spectrum[22]. Beyond fundamental research, solid argon-related materials like argyrodite have shown promise in solid-state batteries, with pressure-tolerant anodes reducing dendrite growth and heat generation, and argon's inertness remains critical in advanced manufacturing processes such as bright annealing of

Received on February 3, 2025; Accepted on March 17, 2025

aerospace alloys, where it preserves material integrity and prevents oxidation.

Based on the coupled cluster singles and doubles with perturbative triples (CCSD(T)) method and the aug-cc-pVQZ basis set, we systematically analyzed the geometric structure and potential energy characteristics of $(Ar)_n$ clusters ($(Ar)_2$ to $(Ar)_5$) in the fcc lattice, and quantified the contributions of many-body interactions to the EOS of solid *Ar*, aiming to provide a more accurate theoretical basis for interpreting high-pressure experimental phenomena. The coupled cluster singles and doubles with perturbative triples (CCSD(T)) method has already been applied in previous studies[3,6,23], and it has been proven to be the most accurate and practical method for studying the properties of dense inert elements.

2 Computational Methods

The total energy of solid *Ar* under different molar volumes was expressed as the sum of many-body interaction energies, and the specific form is shown in the following formula[18]:

$$\begin{aligned} E(V) &= E_2(V) + E_3(V) + \cdots \\ &= \frac{1}{2}U_2(o) + \frac{1}{3}U_3(o) + \cdots \\ &= \frac{1}{2}\sum_{i=1}^{n-1} u_2(o,i) + \frac{1}{3}\sum_{i<j=1}^{n-1} u_3(o,i,j) + \cdots \end{aligned} \quad (1)$$

Where $E_n(V)$ represents the *n*-body interaction energy component related to molar volume *V*, $U_n(o)$ denotes the total *n*-body potential energy centered on atom *o*, and $u_n(o, i, j, \ldots)$ is the *n*-body potential energy function between the central atom *o* and surrounding atoms[18].

The pressure is expressed by:

$$P(V,T) = \sum_{n=2}^{+\infty} P_n(V) + P_{zp}(V) + P_{th}(V,T) \quad (2)$$

The pressure corresponding to many-body term is derived from the partial derivative of the energy with respect to volume:

$$P_n(V) = -\frac{\partial E_n(V)}{\partial V}, (n=2,3,4,\ldots) \quad (3)$$

The thermal pressure of solid *Ar* at finite temperature was calculated using the following formula:

$$P_{th}(V,T) = \frac{\gamma 9 k_B T}{V}\left(\frac{\Theta}{T}\right)^{-3}\int_0^{\Theta/T}\frac{x^3}{e^x - 1}dx, \quad (4)$$

where γ is the *Grüneisen* coefficient, k_B is the Boltzmann constant, Θ is the Debye temperature, and *T* is the absolute temperature.

The zero-point vibrational pressure P_{zp} is given by:

$$P_{zp}(V) = \frac{\gamma}{V}E_{zp}, \quad (5)$$

and the zero-point vibrational energy E_{zp} is:

$$E_{zp} = \frac{9}{8}k_B\Theta \quad (6)$$

3 Calculation Results and Discussion

3.1 Geometric configurations of Ar clusters

Based on the established fcc lattice structure of solid *Ar*[19], it analyzed the properties of Ar_2 to Ar_5 clusters, including geometrical configuration, geometrical parameters. Figure 1 showed some geometric configurations of Ar_5 clusters in fcc lattice. The results showed that, all 12 geometric configurations of $(Ar)_2$ clusters are linear, so their structural diagrams are not separately presented. For $(Ar)_3$ clusters, it have 861 (C^2_{42}) atoms and belong to 25 different geometric configurations, $(Ar)_4$ clusters have 816 (C^3_{18}) atoms and belong to 27 different geometric configurations. For $(Ar)_5$ multiple typical configurations were observed. Detailed structural parameters (such as bond lengths and bond angles) of these clusters were recorded to provide a basis for subsequent potential energy calculations.

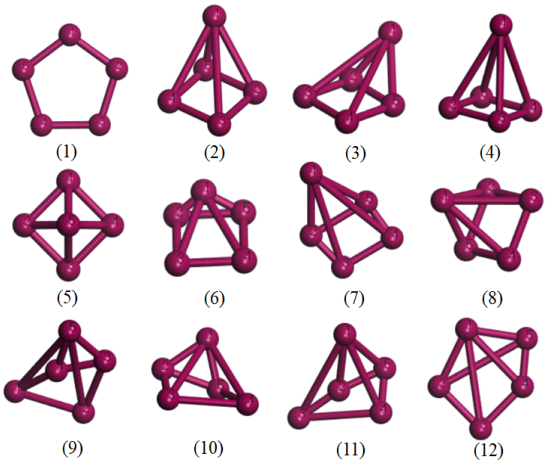

Figure 1 Part of geometric configurations for $(Ar)_5$ clusters in fcc lattice

3.2 Truncation and convergence of many-body potentials

The convergence speed of the many-body expansion series directly affects the computational efficiency of potential energy. For the truncation radius of atomic potentials, the potential energy values tend to stabilize with the increase of the number of neighboring atoms. We analyzed the variation of two-body potential energy $U_2(o)$ and three-body potential energy $U_3(o)$ with the truncation radius at atomic distances of 2.0Å, 2.4Å, 2.7Å, and 3.2Å in the fcc phase, as shown in Figure 2. The results show that when the truncation radius reaches 4.0Å, the two-body and three-body potential energies basically reach saturation, and the number of neighboring atoms corresponding to this radius is 42. Considering the balance between computational accuracy and efficiency, a truncation radius of 4.0Å was selected for subsequent calculations, which can achieve a good approximation effect while avoiding excessive

computational costs. For the atomic distance of 2.0Å, the number of sampling points was set to 200,000 to ensure the reliability of the calculation results.

3.3 Equation of state

In the equation of state calculation, the total pressure $P(V)$ are composed of static pressure P_n, zero-point vibration pressure P_{zp} and thermal pressure P_{th}, which are functions of molar volume V. It was found that the zero-point vibration pressure P_{zp} and thermal pressure P_{th} of solid *Ar* account for less than 5% of the total pressure $P(V)$, but their contributions cannot be ignored in high-precision calculations. This study compared the EOS results of different combinations: the two-, three-, four-body potential pressure, zero-point vibration pressure, thermal pressure ($P_2+P_3+P_4+P_{zp}+P_{th}$), as shown in Figure 3. The results show that, only considering two-body potential, our calculation results are in good agreement with the experimental data[8,20] within a pressure of 15GP. Within the pressure range of 0～80 GPa, the calculation results which considering the two- and three-body potential pressure are in good agreement with the experimental data[8,20]. When the pressure exceeds 80 GPa, the EOS accuracy of the two-, three-body-based combination decreases significantly, while the combination including four-body terms can maintain high precision up to 114 GPa, while the consistency between the calculation results of density functional theory based on the generalized gradient approximation (GGA) and the local-density approximation (LDA) and the experimental data[8,20] in the high-pressure area. Above 114 GPa, the influence of higher-order many-body terms (five-body and above) becomes prominent, and their inclusion is required to accurately interpret the experimental phenomena under ultra-high pressure. In addition, it can be seen from the top right image in Figure 3 that the zero-point vibration pressure and thermal pressure are relatively small, but not negligible within the entire experimental range of pressure.

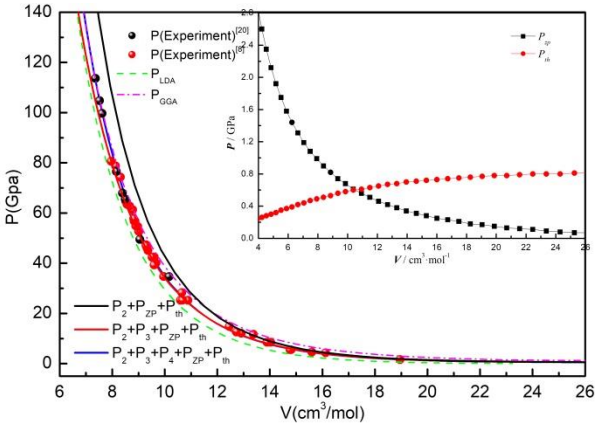

Figure 3 Equation of state for solid *Ar*

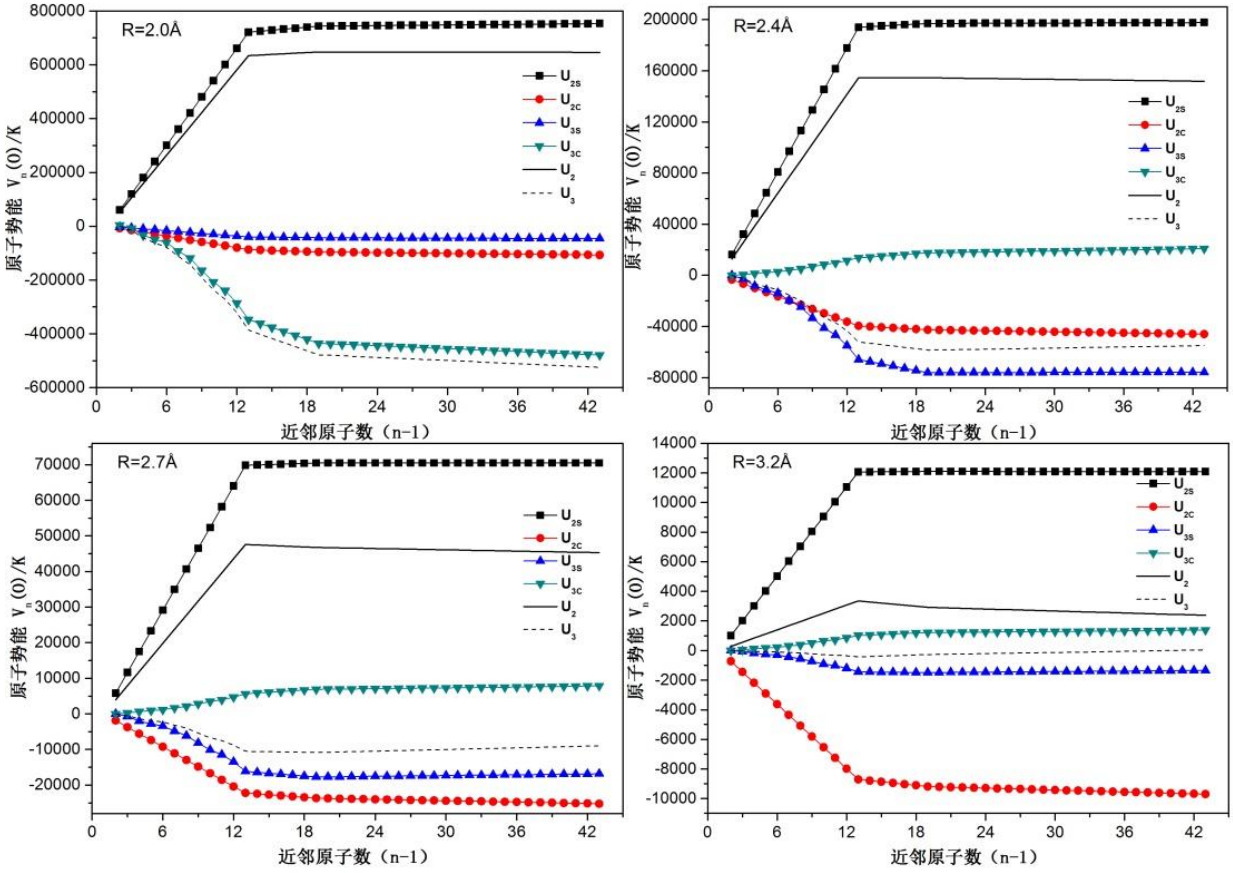

Figure 2 Atomic potential and its many-body components variations with the number of neighbours at R=2.0, 2.4,2.7, 3.2Å in fcc phase

4 Conclusions

Based on the CCSD(T) method and aug-cc-pVQZ basis set, we accurately calculated the two-, three-body and four-body contributions to the cohesive energy and EOS of fcc solid *Ar* within the atomic distance range of 2.0Å to 3.6Å at room temperature (*T*=300 K). The geometric structures of $(Ar)_2$, $(Ar)_3$, $(Ar)_4$, and $(Ar)_5$ clusters in the fcc lattice were clarified, and their symmetry characteristics and structural parameters were analyzed. The truncation radius of 4.0Å was determined through convergence tests, which balances computational efficiency and accuracy. EOS comparison results show that the model including two-body and three-body terms can accurately describe the compression behavior of solid *Ar* within 80 GPa, and the addition of four-body terms extends the applicable pressure range to 114 GPa. To further improve the EOS accuracy above 114 GPa, it is necessary to consider the contribution of higher-order multi-body interactions. Although the zero-point vibration pressure and thermal pressure are relatively small, but not negligible within the entire experimental range of pressure. Especially, when the molar volume is reduced to a fixed value, the zero-point vibration pressure has already reached a certain proportion, then it must be considered. This study provides a reliable theoretical model for the study of high-pressure properties and zero-point energy of rare gas solids.

Acknowledgement: The research are sponsored by the Youth Talent (team) project of Gansu Province (Grant No. 2025QNTD12), the Natural Science Foundation of Gansu Province (Grant No. 25JRRM001, 23JRRM0755).

References

[1] T. W. Maltby, M. Hammer. Equation of State for Solid Argon Valid for Temperatures up to 300 K and Pressures up to 16 GPa [J]. Journal of Physical and Chemical Reference Data, 2024, 53(4):043102.

[2] X. Xiao, S. Sriskandaruban. Equation of State for Solid Argon Valid for Temperatures up to 760 K and Pressures up to 6300 MPa [J]. International Journal of Thermophysics, 2025, 46(1):1-47.

[3] N. Boucerredj, K. Beggas. First Principle Calculation of Electronic and Optical Properties of Rare Gas Solids Kr and Ar [J]. Acta Physica Polonica A, 2020, 138(3):428-433.

[4] T. T. Ha, D. D. Phuong. Investigation of mean-square displacement and elastic moduli of solid argon up to 85 GPa [J]. Chemical Physics, 2020(539):110928.

[5] Y. Liu, L. Zhang. Cryogenic phonon-detector model with solid argon for detecting dark matter [J]. Chinese Physics C, 2023,47(12):5-13.

[6] X. R. Zheng, H. J. Chen. The zero-point vibration contributions to energy and compressibility of light rare-gas solids [J]. Physica B, 2023(669):415268.

[7] V. N. Nguyen, H. H. Khac. Equation-of-state and melting curve of solid neon and argon up to 100 GPa [J]. Vacuum, 2022(196):110725.

[8] D. Errandonea, R. Boehler, S. Japel, M. Mezouar, and L. R. Benedetti. Structural transformation of compressed solid Ar: An x-ray diffraction study to 114 GPa [J]. Phys. Rev. B., 2006,73(9):092106.

[9] Li J H, Zheng X R, Peng C N. Effect of many-body interactions on the equation of state for solid argon [J]. Journal of Sichuan University. 2016,53(1):131-136.

[10] Freiman Y A, Tretyak S M. Many-body interactions and high-pressure equations of state in rare-gas solids [J]. low temperature physics, 2007,33(6-7):545-552.

[11] I. V. Shchus, D. A. Tyurin, V. I. Feldman. Radiation-induced transformations of isolated dimethyl disulphide molecules in solid argon [J]. Radiation Physics and Chemistry, 2024(11):215.

[12] S. G. Boussahoul, M. Benguerba. Modeling of sputtering from solid surfaces under argon cluster bombardments: comparison with experimental and simulated data [J]. Applied Surface Science, 2025(703):163428.

[13] I. S. Sosulin,V. I. Feldman. Infrared spectrum of CF^{2+} cation in a solid argon matrix [J]. Chemical Physics Letters, 2022(807):140108.

[14] E. I. German, S. B. Tsydypov. Structure of Argon Solid Phases Formed from the Liquid State at Different Isobaric Cooling Rates [J]. Applied sciences-basel, 2024,14(3):1295.

[15] S. L. Chou, S. Y. Lin. Infrared absorption spectra of phenoxide anions isolated in solid argon [J]. Journal of the Chinese Chemical Society, 2022,69(1):133-139.

[16] X. R. Zheng, L. Su. The fitting of three-body potential energy of solid argon [J]. Journal of Physics: Conference Series, 2021,1906(1):012011.

[17] M. Miyaji, B. Radola. Extension of Kirkwood-Buff theory to solids and its application to the compressibility of fcc argon [J]. The Journal of chemical physics, 2021,154(16):164506.

[18] A. N. Singh, J. C. Dyre, U. R. Pedersen. Solid-liquid coexistence of neon, argon, krypton, and xenon studied by simulations [J]. The Journal of chemical physics, 2021,154(13):134501.

[19] X. R. Zheng, G. Q. Li. Investigations of crystal configuration and material properties of high-compressed solid argon [J]. Journal of Qinghai University, 2019,37(6):71-79.

[20] A. P. Jephcoat. Rare-gas solids in the Earth's deep interior [J]. Nature, 1998(393):355.

[21] A. A. Adeleke, M. Kunz. A High-Pressure Compound of Argon and Nickel: Noble Gas in the Earth's Core [J]. ACS Earth and Space Chemistry, 2019,3(11):2517-2524.

[22] F. Bouchelaghem, H. Boutarfa. New determination of the thermophysical properties of argon gas considering nuclear spin and symmetry effects [J]. Journal of molecular modeling, 2025,31(8):215.

[23] X. R. Zheng. Higher-term contributions in the many-body calculation of the compressibility and thermodynamic properties of solid neon [J]. Indian Journal of Physics, 2019,93(12):1579-1589.